

## Eliassen-Palm Cross Sections for the Troposphere<sup>1</sup>

H. J. EDMON, JR.<sup>2</sup>

*Joint Institute for the Study of the Atmosphere and Ocean, University of Washington, Seattle 98195*

B. J. HOSKINS

*U.K. Universities' Atmospheric Modelling Group, University of Reading, Reading, England*

M. E. MCINTYRE<sup>3</sup>

*Joint Institute for the Study of the Atmosphere and Ocean, University of Washington, Seattle 98195*

(Manuscript received 30 May 1980, in final form 28 August 1980)

### ABSTRACT

"Eliassen-Palm (EP) cross sections" are meridional cross sections showing the Eliassen-Palm flux  $F$  by arrows and its divergence by contours. For large-scale, quasi-geostrophic motion  $F$  is defined to have  $\varphi$  and  $p$  components  $r_0 \cos\varphi [-\overline{u'v'}, \overline{fv'\theta'}/\theta_p]$ , where  $\varphi$  is latitude,  $p$  pressure,  $\theta$  potential temperature,  $r_0$  the radius of the earth, bars and primes denote zonal means and deviations and  $(u, v)$  is horizontal velocity.

The theoretical reasons for using EP cross sections diagnostically are reviewed. The divergence of  $F$  reflects the magnitude of transient and irreversible eddy processes at each height and latitude, and is proportional to the northward flux of quasi-geostrophic (not Ertel's) potential vorticity. It is a direct measure of the total forcing of the zonal-mean state by the eddies. The direction of  $F$  indicates the relative importance of the principal eddy fluxes of heat and momentum. If the eddy dynamics is Rossby wavelike, then  $F$  is also a measure of net wave propagation from one height and latitude to another.

Observational and theoretical EP cross sections are presented for the layer 1000–50 mb, and discussed in terms of the abovementioned properties. The observational cross sections for transient eddies are more reliably determined than for stationary eddies, and resemble to a significant degree the cross sections given by nonlinear baroclinic instability simulations. They do not resemble those given by linear instability theory for a realistic mean state (verifying the inappropriateness of linear theory as a basis for eddy parameterizations). They provide a direct view of the latitudinal planetary-wave propagation mechanism whereby midlatitudinal instabilities influence the high-tropospheric subtropics. A similar dynamical linkage appears to be depicted by the EP cross sections for stationary eddies in winter. The cross sections for stationary eddies in summer are strikingly different, but not very well determined by the data. Nevertheless, there are reasons why some of the differences might be real, with possible implications for theories of stationary planetary waves. The "residual meridional circulations" associated with the observed EP cross sections are presented and discussed.

### 1. Introduction

The purpose of this paper is to suggest that meridional cross sections displaying the Eliassen-Palm (EP) flux by means of arrows, and its divergence by means of contours, would be useful as a standard diagnostic for disturbances on a mean zonal wind. The relevant theory is reviewed in Sections 2 and 3. Such EP cross sections exhibit the principal eddy heat, momentum and potential-vorticity fluxes in one diagram, making their relative magnitudes and

spatial interrelationships easier to appreciate. They provide a succinct framework for comparing theory, observation and numerical experiment, and for assessing parameterizations of eddy effects. Moreover, the particular combinations of eddy fluxes which are represented on an EP cross section are fundamental for the interaction between eddies and mean state, more so than the eddy heat and momentum fluxes considered separately, and more so than the eddy energy fluxes originally emphasized by Eliassen and Palm themselves. The information displayed on an EP cross section, in fact, may come as near to those fundamentals as is practicable without resorting to a generalized Lagrangian-mean (GLM) description—a matter of some importance in view of the several difficulties in using the GLM theory at large eddy amplitude, which have been discussed

<sup>1</sup> Contribution No. 6, Joint Institute for the Study of the Atmosphere and Ocean, University of Washington/NOAA.

<sup>2</sup> Present affiliation: Dept. of Atmospheric Sciences, AK-40, University of Washington, Seattle 98195.

<sup>3</sup> Present affiliation: Dept. of Applied Mathematics and Theoretical Physics, University of Cambridge, England.

elsewhere (Andrews and McIntyre, 1978b; Dunkerton, 1980; McIntyre, 1980a).

The plan of the paper is as follows. Section 2 gives the theoretical background for quasi-geostrophic dynamics, and points out a nonlinear extension of the Eliassen-Palm theorem. Section 3 gives full details of how to compute EP cross sections for spherical geometry. Sections 4 and 5 present and discuss observational EP cross sections for the layer 1000–50 mb, averaged over winters and summers, and with stationary and transient eddies separately accounted for. The cross sections were compiled from two independent sets of general circulation statistics. The transient eddy cross sections discussed in Section 4 are compared with theoretical EP cross sections for different models of baroclinic instability. Included are cross sections for the life cycle of a nonlinear baroclinic wave similar to that described in Simmons and Hoskins (1978), but starting with a somewhat more realistic mean state. The results remind us sharply of the inadvisability of using linear baroclinic instability theory as a basis for parameterizing the effects of eddies on the mean state.

Section 5 discusses the very different EP signatures obtained for stationary eddies in winter and summer. Section 6 uses the transformed Eulerian-mean equations presented by Andrews and McIntyre (1976, 1978a) to depict the maintenance of the general circulation in terms of the EP flux divergence and the induced ‘‘residual meridional circulation.’’

In Section 7 we point out a practical dilemma concerning the choice of arrow scales when EP cross sections are to be extended far into the stratosphere. Despite this, the cross sections and the transformed mean-flow equations are being found useful in observational and modeling studies of the stratosphere and mesosphere, as is amply demonstrated in forthcoming papers by Dunkerton *et al.* (1980), Holton and Wehrbein (1980), Palmer (1980) and Sato (1980). The modeling studies illustrate with special clarity the power of the EP concepts as used here, which are quite independent of whether or not the eddies conform to the original assumptions made by Eliassen and Palm.

In Section 8 we conclude by suggesting some modeling studies which we think would be of particular interest for the troposphere.

## 2. Theory

### a. The Eliassen-Palm theorem and the transformed mean-flow equations

In their celebrated paper Eliassen and Palm (1961) presented a basic theorem for wavelike disturbances to a zonal mean wind  $\bar{u}$  with arbitrary horizontal and vertical shear. The theorem is expressed in terms of a vector quantity  $\mathbf{F}$  lying in a meridional

plane, involving the northward eddy fluxes of heat and angular momentum. In the case of beta-plane geometry with pressure  $p$  as vertical ‘‘coordinate,’’  $\mathbf{F}$  is given in the quasi-geostrophic approximation by

$$\mathbf{F} = \{F_{(y)}, F_{(p)}\},$$

where

$$F_{(y)} = -\overline{v'u'}, \tag{2.1a}$$

$$F_{(p)} = f\overline{v'\theta'}/\bar{\theta}_p. \tag{2.1b}$$

Overbars and primes denote zonal means and departures therefrom,  $y$  is northward distance,  $u$  and  $v$  are zonal and meridional velocity,  $f = f(y)$  is the Coriolis parameter, and  $\theta$  is potential temperature. Subscripts without parentheses denote partial differentiation so that  $-\bar{\theta}_p$  measures the static stability, the corresponding buoyancy frequency being

$$N = (-\bar{\rho}g^2\bar{\theta}_p/\bar{\theta})^{1/2},$$

where  $\rho$  is density. For the generalization of (2.1) to the ageostrophic case, see EP; for spherical geometry see Andrews and McIntyre (1976), Boyd (1976) and Section 3 below.  $\mathbf{F}$  has no established name; we shall simply call it the Eliassen-Palm flux to avoid any preconception as to its physical interpretations. The Eliassen-Palm theorem states that the divergence of  $\mathbf{F}$ ,

$$\nabla \cdot \mathbf{F} \equiv \frac{\partial F_{(y)}}{\partial y} + \frac{\partial F_{(p)}}{\partial p}, \tag{2.2}$$

is zero for steady, conservative, wavelike disturbances of the zonal wind. This property sharply distinguishes  $\mathbf{F}$  from other diagnostics such as eddy energy fluxes, and suggests that for some purposes  $\mathbf{F}$  and  $\nabla \cdot \mathbf{F}$  should be regarded as more fundamental than those other diagnostics.

That idea receives further support from two distinct bodies of theory. The first of these concerns the effect of the eddies on the zonal-mean state, and the second relates to the concepts of wave action and group velocity.

The relationship between  $\mathbf{F}$  and the effect of the eddies on the zonal-mean state, first recognised by Charney and Drazin (1961), is easiest to see from the the transformed mean-flow equations presented by Andrews and McIntyre (1976, Section 3). The transformed mean-flow equations reduce in the quasi-geostrophic approximation to

$$\partial \bar{u} / \partial t - f \bar{v}^* - \bar{\mathcal{F}} = \nabla \cdot \mathbf{F}, \tag{2.3a}$$

$$f \bar{u}_p - R \bar{\theta}_y = 0, \tag{2.3b}$$

$$\bar{v}_y^* + \bar{\omega}_p^* = 0, \tag{2.3c}$$

$$\partial \bar{\theta} / \partial t + \bar{\theta}_p \bar{\omega}^* - \bar{\mathcal{Q}} = 0, \tag{2.3d}$$

where overbars denote zonal means as before,  $\bar{\mathcal{F}}$  and  $\bar{\mathcal{Q}}$  are the Eulerian-mean friction and heating,  $R$  is the gas constant times  $(p_0/p)^{1/\gamma} p_0^{-1}$  ( $\gamma$  being the

ratio of specific heats), and  $(\bar{v}^*, \bar{\omega}^*)$  is a "residual meridional circulation" defined by

$$\bar{v}^* = \bar{v} - \partial(\overline{v'\theta'}/\bar{\theta}_p)/\partial p, \quad (2.4a)$$

$$\bar{\omega}^* = \bar{\omega} + \partial(\overline{v'\theta'}/\bar{\theta}_p)/\partial y, \quad (2.4b)$$

Eqs. (2.3a,d) are simple to derive, by using (2.4) to eliminate  $\bar{v}$  and  $\bar{\omega}$  from the usual equations for  $\partial\bar{u}/\partial t$  and  $\partial\bar{\theta}/\partial t$ . We have used standard scaling arguments to neglect ageostrophic terms, particularly terms on the right-hand sides of Andrews and McIntyre's Eqs. (3.5b,d), and  $\bar{v}^*\bar{\theta}_y$ ,  $\bar{v}^*\bar{u}_y$  and  $\bar{\omega}^*\bar{u}_p$ .

Eqs. (2.3) comprise a complete set of equations for the mean state described in terms of the quantities  $\{\bar{u}, \bar{v}^*, \bar{\omega}^*, \bar{\theta}\}$ . They show that within the quasi-geostrophic approximations  $\nabla \cdot \mathbf{F}$  represents the sole internal forcing of the mean state by the disturbances. In particular, there are no eddy-heat-flux terms on the right of (2.3d). Note that if  $\nabla \cdot \mathbf{F}$ ,  $\bar{\mathcal{F}}$ , and  $\bar{\mathcal{Q}}$  all vanish, the equations permit a steady mean state in which  $\bar{u}_t$ ,  $\bar{\theta}_t$ ,  $\bar{v}^*$  and  $\bar{\omega}^*$  are all zero; this is Charney and Drazin's "nonacceleration theorem." However, the transformed equations themselves do not depend on how closely the conditions of the Eliassen-Palm and Charney-Drazin theorems hold. In fact, the equations can provide an extremely useful view of the mean dynamics under conditions far removed from those of the theorems, such as are encountered, for example, in sudden stratospheric warmings (Dunkerton *et al.*, 1980; Holton and Wehrbein, 1980; Palmer, 1980).

The absence of eddy heat flux terms in (2.3d) suggests that the residual circulation  $(\bar{v}^*, \bar{\omega}^*)$  has properties similar in some respects to those of a Lagrangian-mean circulation. The conditions under which such a relationship can be expected have been discussed in another context by Dunkerton (1978). Residual and Lagrangian-mean circulations cannot, of course, be the same thing generally, as Andrews and McIntyre (1976, Section 6c) are careful to point out. The residual circulation is a strictly Eulerian diagnostic. Its observed seasonally averaged form for the troposphere is discussed in Section 6.

From (2.3c) a streamfunction  $\bar{\psi}^*$  for the residual circulation may be introduced. Then  $-f(\partial/\partial p)$  of (2.3a) plus  $R(\partial/\partial y)$  of (2.3d) gives an equation for this streamfunction:

$$f^2 \bar{\psi}_{pp}^* + R[\theta_p \bar{\psi}_{yy}^*]_y = -f(\nabla \cdot \mathbf{F})_p - f \bar{\mathcal{F}}_p + R \bar{\mathcal{Q}}_y.$$

This is equivalent to the equation of Eliassen (1952) for the usual Eulerian-mean meridional circulation. It shows the circulation necessary to maintain geostrophic balance in the presence of  $\nabla \cdot \mathbf{F}$ , frictional and diabatic effects. Neglecting the last two forcings

and boundary effects, the  $\bar{\psi}_{pp}^*$  term will tend to dominate when  $\nabla \cdot \mathbf{F}$  has a meridional scale much larger than a radius of deformation. Note that there can then be complete cancellation between  $-f\bar{v}^*$  and  $\nabla \cdot \mathbf{F}$  in (2.3a), if the integral of  $\nabla \cdot \mathbf{F}$  with respect to  $p$  is small. If the integral is not small, substantial mean accelerations can still occur; an example is discussed in detail in Dunkerton *et al.* (1980). In steady-state or long-term average conditions it is easier to argue directly from (2.3a) and (2.3d) with the tendency terms omitted.

### b. Quasi-geostrophic potential vorticity theory

An alternative but less direct way of seeing the relationship between  $\mathbf{F}$  and the eddy-induced forcing of the mean state is through the quasi-geostrophic potential-vorticity theory (Charney and Stern, 1962; Bretherton, 1966; Dickinson, 1969; Green, 1970; Geisler, 1974; Rhines, 1977; Holton and Dunkerton, 1978; Rhines and Holland, 1979).  $\nabla \cdot \mathbf{F}$  is related to the northward quasi-geostrophic potential-vorticity flux in a well-known way, and hence (Dickinson, 1969) to the equation governing the zonal mean of the quasi-geostrophic potential vorticity  $q$ . For the beta-plane the relationship is simply

$$\nabla \cdot \mathbf{F} = \overline{v'q'}, \quad (2.5)$$

the quasi-geostrophic eddy potential vorticity  $q'$  being defined as

$$q' = v_x' - u_y' + f(\theta'/\bar{\theta}_p)_p. \quad (2.6)$$

As is shown, for example, in Green (1970), relation (2.5) follows from (2.1) in a line or two of manipulation provided we assume that  $v'$  satisfies the thermal wind relation in the form  $v_p' \propto \theta_x'$  at given  $(\varphi, p)$ , where  $x$  is the zonal coordinate, and that

$$\nabla_H \cdot \mathbf{u}' \equiv u_x' + v_y' = 0, \quad (2.7)$$

as is true to leading order for quasi-geostrophic motion. A result corresponding to (2.5) for the barotropic case was given by Taylor (1915).

One reason why the relation (2.5) is important in practice is that we can often use it to anticipate the sign of  $\nabla \cdot \mathbf{F}$  (e.g., Rhines and Holland, 1979). If quasi-geostrophic eddies are causing irreversible, north-south dispersion of air parcels [and if the associated potential-entropy cascade is the main process controlling eddy dissipation—see Rhines (1977)], then we would expect the flux  $\overline{v'q'}$  averaged over an eddy lifetime to be downgradient. This gives its sign if the local mean gradient

$$\bar{q}_y \equiv \beta - \bar{u}_{yy} + f(\bar{\theta}_y/\bar{\theta}_p)_p \quad (2.8)$$

is of known sign. Here  $\beta$  is the planetary vorticity gradient, and the last term relates to vortex stretching associated with the variation of isentropic slopes with altitude. If  $\bar{q}_y$  is positive (northward), as it is

<sup>4</sup> Note added in proof: The model is not quite the same as Charney's, having an upper lid at one scale height. None of the discussion is affected.

when  $\beta$  dominates, then a downgradient quasi-geostrophic potential-vorticity flux would be southward, giving negative  $\nabla \cdot \mathbf{F}$ .

We emphasize that it is the flux of quasi-geostrophic potential vorticity which tends to be downgradient, rather than the flux of Ertel's potential vorticity studied (e.g., Hartmann, 1977; Lau, 1978; Lau and Wallace, 1979). The distinction between the horizontal fluxes of quasi-geostrophic and Ertel's potential vorticity on an isobaric surface [or, almost equivalently, between the *isentropic* and isobaric fluxes of Ertel's potential vorticity—see Charney and Stern's (1962) Eq. (2.31)] is significant in a strongly stratified atmosphere because of the role of vertical advection in Ertel's theorem. Only horizontal advection, by the geostrophic wind, is involved in Charney and Stern's conservation theorem for the quasi-geostrophic potential vorticity [Eq. (2.9) below]. The isobaric flux of Ertel's potential vorticity can be upgradient in a stratified atmosphere in just the same way as the corresponding eddy flux of heat; the kinematics involved is elegantly discussed in Wallace (1978), Plumb (1979) and Matsuno (1980).

c. A nonlinear extension of the Eliassen-Palm theorem

Another important consequence of (2.5) is that the EP theorem ( $\nabla \cdot \mathbf{F} = 0$ ) holds for quasi-geostrophic disturbances of finite amplitude, under nonacceleration conditions. This result goes beyond the original, linear result (albeit ageostrophic) proved by EP and does not seem to have been explicitly pointed out before, perhaps because the proof, although simple, is less direct and requires slightly different hypotheses. (The need for different hypotheses is inevitable, because at finite amplitude the eddies cannot be treated independently of their effects on the mean state as in EP.)

"Nonacceleration conditions" in general mean (i) strictly conservative eddy and mean-flow dynamics, (ii) constant eddy amplitude, measured in a Lagrangian sense involving north-south air parcel displacements, and (iii) steady mean flow, in both the Eulerian and Lagrangian senses. Andrews and McIntyre (1978b, Section 5) showed quite generally that (iii) is possible given (i) and (ii). The simplest proof of the nonlinear, quasi-geostrophic EP theorem takes condition (iii) as its starting point (in fact, only steadiness of the Eulerian-mean flow is used), and assumes in addition that  $\overline{v'q'}$  vanishes at the pole or, for the beta-plane, at a channel wall at some latitude  $y = y_N$ , say.

If the motion is quasi-geostrophic, we have conservation of  $q$  (Charney and Stern, 1962), i.e.,

$$\begin{aligned} 0 &= q_t + uq_x + vq_y \\ &= q_t + (uq)_x + (vq)_y. \end{aligned} \tag{2.9}$$

The equivalence between the first and second lines depends on the analog of (2.7),

$$\nabla_H \cdot \mathbf{u} \equiv u_x + v_y = 0,$$

for the total geostrophic wind  $(u, v)$ . [Evaluation of  $q = \bar{q} + q'$  in (2.9) involves integrating (2.8) with respect to  $y$ : the constant of integration should not be taken too large if the second line of (2.9) is to conform to quasi-geostrophic scaling.] Now since  $v$  in (2.9) is the northward geostrophic wind, by definition (Charney and Stern, 1962), it is proportional to the  $x$  derivative of the geopotential and so has zonal mean exactly zero. Therefore  $\overline{vq} = \overline{v'q'} = \overline{v'q'}$ , and (2.9) implies that

$$\bar{q}_t + (\overline{v'q'})_y = 0. \tag{2.10}$$

Under nonacceleration conditions the mean state is steady, and in particular  $\bar{u}$  and  $\bar{\theta}$  are constant in time. Therefore,  $\bar{q}$  is likewise constant. [The argument makes no reference here to the eddy quantities  $u'$ ,  $v'$  and  $\theta'$ , because by (2.6) they appear linearly in  $q$  and so make no contribution to  $\bar{q}$ .] It then follows from (2.10) that  $\overline{v'q'}$  is independent of latitude. If  $\overline{v'q'}$  is assumed to vanish at latitude  $y = y_N$ , we have finally

$$\overline{v'q'} = \nabla \cdot \mathbf{F} = 0 \tag{2.11}$$

at all latitudes.

Reliance on the boundary condition at  $y = y_N$  can be dispensed with if we make alternative but somewhat more restrictive hypotheses. On any given isobaric surface, assume first that there is a band of latitudes within which the total flow (mean flow plus eddies) is strictly steady in some frame of reference. This is possible if all the eddies have exactly the same zonal phase speed, as was originally assumed by EP. Second, assume that on the given isobaric surface there is a geopotential height contour  $C$  which lies within the hypothesized latitude band and divides it into a northern part and a southern part. By hypothesis, the total flow is steady within the area  $A$  enclosed between  $C$  and some latitude circle  $L$ . Therefore the total amount of  $q$  within  $A$  is constant. There can be no geostrophic transport of  $q$  across  $C$ , since it is a steady streamline for the geostrophic wind. Integration of (2.9) over  $A$  therefore shows that  $\overline{vq}$  is zero on  $L$ , and the result (2.11) follows as before.

Neither proof of the nonlinear EP theorem depends on any assumption about the boundary conditions on the residual circulation [as would a proof proceeding from Eqs. (2.3)]. Nor do the proofs depend on whether or not there are critical or steering levels within the domain under consideration. This accords with the fact that conservative dynamics and steady Eulerian-mean flow are perfectly possible at a critical level, as is shown for instance by the steady "cat's eye" solutions found by Benney and Bergeron (1969) and Davis (1969).

#### d. Wave theory

The second body of theory, tending to support the view that  $\mathbf{F}$  and  $\nabla \cdot \mathbf{F}$  should be regarded as fundamental diagnostics in their own right, is that relating to the wave-action and group velocity concepts. An introduction to the main ideas has been given elsewhere (McIntyre, 1980b); the central point is that whenever the eddy dynamics is wavelike (which in this context means describable by linear planetary-wave theory),  $\mathbf{F}$  may be regarded as a measure of the net rate of transfer of wave activity from one latitude and height to another. This idea is justified by the appearance of  $\mathbf{F}$  as the flux in a conservation equation, valid for linear, conservative waves on a steady zonal flow in which no conversion terms representing exchanges with the mean state appear. That conservation equation is in turn a special case of the "generalized Eliassen-Palm relation" derived by Andrews and McIntyre (1976, 1978a), which has the form

$$\frac{\partial A}{\partial t} + \nabla \cdot \mathbf{F} = D, \quad (2.12)$$

where  $D$  is zero for conservative motion (no dissipation or generation of the waves by diabatic or frictional effects), and  $A$  can be regarded as a conserved measure of local wave activity by virtue of its role as the density in the conservation equation to which (2.12) reduces when its right-hand side is zero. For want of a better name we shall simply call  $A$  the density of "EP wave activity"; it is related, but not equal, to the wave-action (whose conservation does not depend on steadiness of the mean flow). In the beta-plane, quasi-geostrophic case an approximate expression for it is

$$A \approx \frac{1}{2} \bar{q}^2 / \bar{q}_y, \quad (2.13)$$

provided that dissipation and nonlinearity are not too strong, and provided that  $\bar{q}_y$  does not vanish. If dissipation is zero it is easy to see where (2.13) comes from. The linearized equation governing  $q'$  is

$$q_t' + \bar{u}q_x' + v\bar{q}_y = 0; \quad (2.14)$$

multiplying by  $q'$ , taking the zonal average, dividing by  $\bar{q}_y$  and using (2.5) immediately gives (2.12) with  $D = 0$  and  $A$  given by (2.13) (Holton and Dunkerton, 1978). If  $\bar{q}_y$  does vanish somewhere, then (2.13) should be replaced by the analogous formula using the disturbance-associated northward particle displacement  $\eta'$ , viz.,

$$A \approx \frac{1}{2} \bar{q}_y \bar{\eta}'^2. \quad (2.15)$$

The appearance of expressions like (2.15) in the theory is related of course to the connection between potential-vorticity fluxes and air parcel dispersion already discussed. An alternative derivation of (2.15), its generalizations when dissipation is impor-

tant, and a corresponding expression for  $D$ , can be obtained from the full ageostrophic forms of  $A$  and  $D$  [Andrews and McIntyre (1976), Eq. (5.5a)]. [One first substitutes Eq. (6.24) of that paper into the expression for  $A$ , and then applies standard quasi-geostrophic scaling as before. The result for  $A$  is minus the right-hand side of (6.2) of McIntyre (1980b).] Eq. (2.15) suggests that wave amplitude is often best thought of for qualitative purposes as proportional to north-south air parcel displacement rather than eddy velocity or geopotential.

The connection between  $\mathbf{F}$  and group velocity theory can be established by standard methods. If one is dealing with planetary waves of small enough latitudinal and vertical wavelength for JWKB or wavepacket theory to be applicable [and, therefore, the group-velocity concept (e.g., Lighthill, 1978)] then it can be shown that

$$\mathbf{F} = c\mathbf{A}, \quad (2.16)$$

where  $c$  is the local group velocity projected onto the meridional plane. The most elementary proof is by straightforward calculation from the three-dimensional, quasi-geostrophic plane-wave solutions for the local mean state treated as if uniform. A more elegant proof proceeds direct from (2.12) following an argument given by Hayes (1977).

The relation (2.16) shows that  $\mathbf{F}$  is parallel to the meridional projection of  $c$ , under conditions for which  $c$  is meaningful. But  $\mathbf{F}$  itself is well defined for any wavelength. It is not, of course, the only general conserved measure of wave-activity flux. Conservation relations like (2.12) suffer from a well-known nonuniqueness: one can for instance add the time derivative of an arbitrary vector to  $\mathbf{F}$ , and subtract its divergence from  $A$ , without affecting (2.12). However, not all the alternatives satisfy (2.16) (cf. the example in Longuet-Higgins, 1964); and  $\mathbf{F}$  does in any case appear to be the most convenient choice to compute from observations.

It will have been noted that the EP wave activity  $A$  is not a positive definite quantity, unless  $\bar{q}_y$  is positive everywhere. This is necessary in order that shear flows shall have their well-known instability properties (D. G. Andrews, personal communication). The present sign convention [which differs from that in McIntyre (1980b)] was chosen to make  $A$  positive for quasi-geostrophic planetary waves when  $\bar{q}_y$  has its usual, positive sign. For such waves, the sense of an arrow representing  $\mathbf{F}$  gives the sense of the group velocity when the idea of group velocity is applicable.

#### e. Summary

An EP cross section displays the following dynamical information about the eddies. To the extent that their dynamics is Rossby wavelike, with  $\bar{q}_y$  positive,

the pattern of arrows representing  $\mathbf{F}$  is a convenient measure of net propagation from one height and latitude to another. The contours of  $\nabla \cdot \mathbf{F}$  represent a zonal force on the mean state comprising the total effect of the eddies in Eqs. (2.3); this holds for all quasi-geostrophic eddies whether linear or non-linear, steady or transient, wavelike or turbulent. Relation (2.5) shows that the contours of  $\nabla \cdot \mathbf{F}$  are also contours of the northward eddy flux of quasi-geostrophic potential vorticity. And when the eddies are so strongly turbulent or dissipative that the wave propagation mechanism is quite ineffective (Rhines, 1977), the tilt of the arrows representing  $\mathbf{F}$  is still informative because it compares the relative magnitudes of the eddy heat and momentum fluxes in a way that is meaningful for quasi-geostrophic dynamics.

3. Data sources and graphical conventions

The transient and standing eddy statistics and mean fields necessary for calculating seasonal averages of the EP flux  $\mathbf{F}$  were taken from two independent sources. The first source is Oort and Rasmusson (1971). The data base for these statistics consists of station data for the period June 1958–May 1963. Eddy and time-mean statistics were computed at each station for the four seasons, and zonal means were calculated. For these statistics winter is defined as December–February and summer is defined as June–August. Statistics are given at 11 pressure levels (1000, 950, 900, 850, 700, 500, 400, 300, 200, 100 and 50 mb) and at every 5° of latitude from 10°S to 75°N.

The second set of statistics is derived from twice-daily National Meteorological Center (NMC) analyses for the Northern Hemisphere at ten pressure levels (1000, 850, 700, 500, 400, 300, 250, 200, 150 and 100 mb) for the 11 winters from 1965–66 to 1975–76 and the 12 summers from 1966 to 1977. In this data set winter is defined as the 120-day period starting from 15 November, and summer as the 120-day period starting from 1 June. Statistics were calculated at each grid point in the NMC octagonal grid, interpolated to a 2.5° latitude by 5° longitude grid starting at 20°N, and zonally averaged. Further information on the winter data as well as other results derived from them may be found in Blackmon (1976), Blackmon *et al.* (1977), Lau *et al.* (1978), Lau (1978, 1979a,b) and Lau and Wallace (1979); the summer data was kindly made available by G. H. White.

To compute EP cross sections for the real atmosphere we need the formulas appropriate to spherical geometry. In place of (2.1) we define

$$F_{(\phi)} = -r_0 \cos\phi \overline{v'u'}, \tag{3.1a}$$

$$F_{(p)} = fr_0 \cos\phi \overline{v'\theta'/\bar{\theta}_p}, \tag{3.1b}$$

where  $\phi$  is latitude,  $r_0$  is the radius of the earth, and

$f$  is now  $2\Omega \sin\phi$  where  $\Omega$  is the earth's angular velocity;  $\bar{\theta}_p$  is also taken as a function of latitude. A latitude dependence consistent with local quasi-geostrophic dynamics would be such that the relative changes  $\Delta\bar{\theta}_p/\bar{\theta}_p$  and  $\Delta f/f$  over an eddy radius are small of the order of the Rossby number. The divergence (2.2) is replaced by

$$\nabla \cdot \mathbf{F} = \frac{1}{r_0 \cos\phi} \frac{\partial}{\partial\phi} (F_{(\phi)} \cos\phi) + \frac{\partial}{\partial p} (F_{(p)}) \tag{3.2}$$

(Andrews and McIntyre, 1976; Boyd, 1976). The transformed mean equations (2.3) are replaced by

$$\partial\bar{u}/\partial t - f\bar{v}^* - \bar{\mathcal{F}} = (r_0 \cos\phi)^{-1} \nabla \cdot \mathbf{F}, \tag{3.3a}$$

$$f\bar{u}_p - R\bar{\theta}_\phi/r_0 = 0, \tag{3.3b}$$

$$(r_0 \cos\phi)^{-1} (\bar{v}^* \cos\phi)_\phi + \bar{\omega}_p^* = 0, \tag{3.3c}$$

$$\partial\bar{\theta}/\partial t + \bar{\theta}_p \bar{\omega}^* - \bar{\mathcal{Q}} = 0. \tag{3.3d}$$

(Andrews and McIntyre, 1978a), the definition (2.4) of the residual meridional circulation by

$$\bar{v}^* = \bar{v} - \frac{\partial}{\partial p} \left( \frac{\overline{v'\theta'}}{\bar{\theta}_p} \right), \tag{3.4a}$$

$$\bar{\omega}^* = \bar{\omega} + \frac{1}{r_0 \cos\phi} \frac{\partial}{\partial\phi} \left( \frac{\overline{v'\theta' \cos\phi}}{\bar{\theta}_p} \right), \tag{3.4b}$$

the relation (2.5) to the quasi-geostrophic potential vorticity flux by

$$\nabla \cdot \mathbf{F} = (r_0 \cos\phi) \overline{v'q'}, \tag{3.5}$$

Eq. (2.6) by

$$q' = (r_0 \cos\phi)^{-1} \{v'_\lambda - (u' \cos\phi)_\phi\} + f(\theta'/\bar{\theta}_p)_p, \tag{3.6}$$

$\lambda$  being longitude, Eq. (2.7) by

$$\nabla_H \cdot \mathbf{u}' \equiv (r_0 \cos\phi)^{-1} \{u'_\lambda + (v' \cos\phi)_\phi\} = 0, \tag{3.7}$$

and Eq. (2.8) by

$$\bar{q}_\phi = 2\Omega \cos\phi - \{(r_0 \cos\phi)^{-1} (\bar{u} \cos\phi)_\phi\}_\phi + f(\bar{\theta}_\phi/\bar{\theta}_p)_p, \tag{3.8}$$

where the notation  $q_\phi$  is chosen to be reminiscent of (2.8) but represents a true derivative with respect to  $\phi$  only within the local quasi-geostrophic approximations. [The global non-integrability of (3.8) comes, again, from the fact that we are working in isobaric and not isentropic coordinates.]

Defining the Eulerian-mean angular momentum  $M$  per unit mass as

$$M \equiv r_0 \bar{u} \cos\phi + r_0^2 \Omega \cos^2\phi,$$

we have the angular momentum principle

$$\frac{\partial M}{\partial t} + \frac{\bar{v}^*}{r_0} M_\phi - r_0 \cos\phi \cdot \bar{\mathcal{F}} = \nabla \cdot \mathbf{F} \tag{3.9}$$

[it differs from  $r_0 \cos\varphi$  times (3.3a) by terms of ageostrophic order]. The connection with angular momentum is the easiest way of seeing why the moment arm  $r_0 \cos\varphi$  appears as a factor in (3.1), in addition to the geometrical scale factor  $\cos\varphi$  appearing in the divergence (3.2). The generalized Eliassen-Palm relation (2.12) for spherical geometry is just  $r_0 \cos\varphi$  times Eq. (5.9a) of Andrews and McIntyre (1976) or Eq. (3.12a) of Andrews and McIntyre (1978a).

The following conventions for representing  $\mathbf{F}$  and its divergence pictorially will be adopted. The mass element for integrating (3.2) over a zonally symmetric portion of the atmosphere is the "volume" element in pressure coordinates divided by the gravitational acceleration  $g$ , viz.,

$$dm = 2\pi r_0^2 g^{-1} \cos\varphi d\varphi dp. \quad (3.10)$$

From (3.2) and (3.10),

$$\int \nabla \cdot \mathbf{F} dm = \int \Delta d\varphi dp, \quad (3.11)$$

where

$$\Delta = \frac{\partial}{\partial\varphi} (2\pi r_0^2 g^{-1} \cos\varphi F_{(\varphi)}) + \frac{\partial}{\partial p} (2\pi r_0^2 g^{-1} \cos\varphi F_{(p)}). \quad (3.12)$$

Thus  $\Delta$  is the natural form of the divergence of  $\mathbf{F}$  for contouring in the  $(\varphi, p)$  plane, since by (3.11) the volume between that plane and a surface at distance  $\Delta$  from it equals  $\int \nabla \cdot \mathbf{F} dm$ . In other words,  $\Delta d\varphi dp$  is the divergence of  $\mathbf{F}$  weighted by the mass  $dm$  of an annular ring  $d\varphi dp$ . Similarly, if arrows are drawn whose horizontal and vertical components are proportional to the differentiated quantities  $\hat{F}_{(\varphi)}$ ,  $\hat{F}_{(p)}$ , say, appearing in (3.12), viz.,

$$\{\hat{F}_{(\varphi)}, \hat{F}_{(p)}\} \equiv 2\pi r_0^2 g^{-1} \cos\varphi \{r_0^{-1} F_{(\varphi)}, F_{(p)}\}, \quad (3.13)$$

expressed in terms of the scale units for  $\varphi$  and  $p$  in the diagram, then the resulting pattern of arrows (centered on an appropriate set of grid points) is the appropriate pattern for representing  $\mathbf{F}$  graphically in the  $(\varphi, p)$  plane. By (3.12), the pattern will look nondivergent in that plane if and only if  $\nabla \cdot \mathbf{F}$  is zero. [Note incidentally that the sign of  $F_{(p)}$  is positive when an arrow points towards high  $p$ , i.e., downward; note also that  $\hat{\theta}_p$  is negative for a statically stable atmosphere.] For wavelike eddy dynamics, the expressions (3.13), when multiplied by  $dp$  and  $d\varphi$ , respectively, give a measure of the total flux of wave activity across an annular, ribbonlike surface bounded by two latitude circles, at  $\{\varphi, p\}$  and  $\{\varphi, p + dp\}$  in the case of  $\hat{F}_{(\varphi)}$ , and at  $\{\varphi, p\}$  and  $\{\varphi + d\varphi, p\}$  in the case of  $\hat{F}_{(p)}$ .

Since (3.11) has the dimensions of torque or energy,  $\Delta$  has dimensions of energy/pressure, or

length cubed, as does  $\hat{F}_{(\varphi)}$ . SI units will be used, so that pressure will be in Pa,  $\Delta$  in  $\text{m}^3$ , and  $\{\hat{F}_{(\varphi)}, \hat{F}_{(p)}\}$  in  $\text{m}^3 \{\text{rad}, \text{Pa}\}$ . (Recall that 1 mb = 100 Pa.) To calculate the horizontal and vertical arrow components as measured on the diagram, the numerical values of  $\hat{F}_{(\varphi)}$  and  $\hat{F}_{(p)}$  are multiplied respectively by the distances occupied by 1 radian of latitude and 1 pascal of pressure on the diagram. This determines the arrow directions uniquely, once the latitude and pressure scales have been chosen. The arrow lengths are determined up to a single constant of proportionality, which is chosen arbitrarily for graphical convenience.

The EP cross sections were calculated from Eqs. (3.1), (3.2), (3.12) and (3.13) using simple centered differences, except at the top and bottom levels where one-sided differences were used. It should be borne in mind that some of the properties of  $\mathbf{F}$  discussed in Section 2 fail to apply near the equator, because quasi-geostrophic theory breaks down there—although  $F_{(\varphi)}$  can still describe horizontal, cross-equatorial Rossby-wave fluxes. We have not attempted to include ageostrophic corrections; a self-consistent set of corrections would involve  $\overline{w'u'}$ , values of which were not available. The ageostrophic corrections to (3.1) and (3.2) were small, however, in the nonlinear baroclinic-wave simulations to be described shortly (despite the fact that the nonlinear development of the simulated baroclinic waves did itself depend on ageostrophic effects, such as changes in static stability due to vertical eddy heat fluxes (see Simmons and Hoskins, 1978, p. 422)).

#### 4. Transient eddies, and remarks concerning parameterization schemes

Figs. 1a and 1b show EP cross sections for transient eddies, calculated from the two different sets of winter statistics (11-year average on the left and Oort and Rasmusson on the right). The analyses stop at 70°N since the flux and its divergence are small north of this latitude for the 11-year-average winter, and since the values in Oort and Rasmusson (1971) stop at 75°N. The analysis from the 11-year set of winter statistics (Fig. 1a) does not extend below 850 mb since the NMC analysis scheme produces nearly geostrophic winds at 1000 mb, which leads to an overestimate of the surface heat flux. A certain amount of confidence can be placed in the results since the two independent sets of circulation statistics yield similar numerical values and spatial patterns. The corresponding cross sections for summer are given in Figs. 1c and 1d. Here there is less agreement between the two data sets. This may be due to the numerical values being smaller and the data consequently less reliable. On the other hand, the patterns do not look obviously noisy, and the

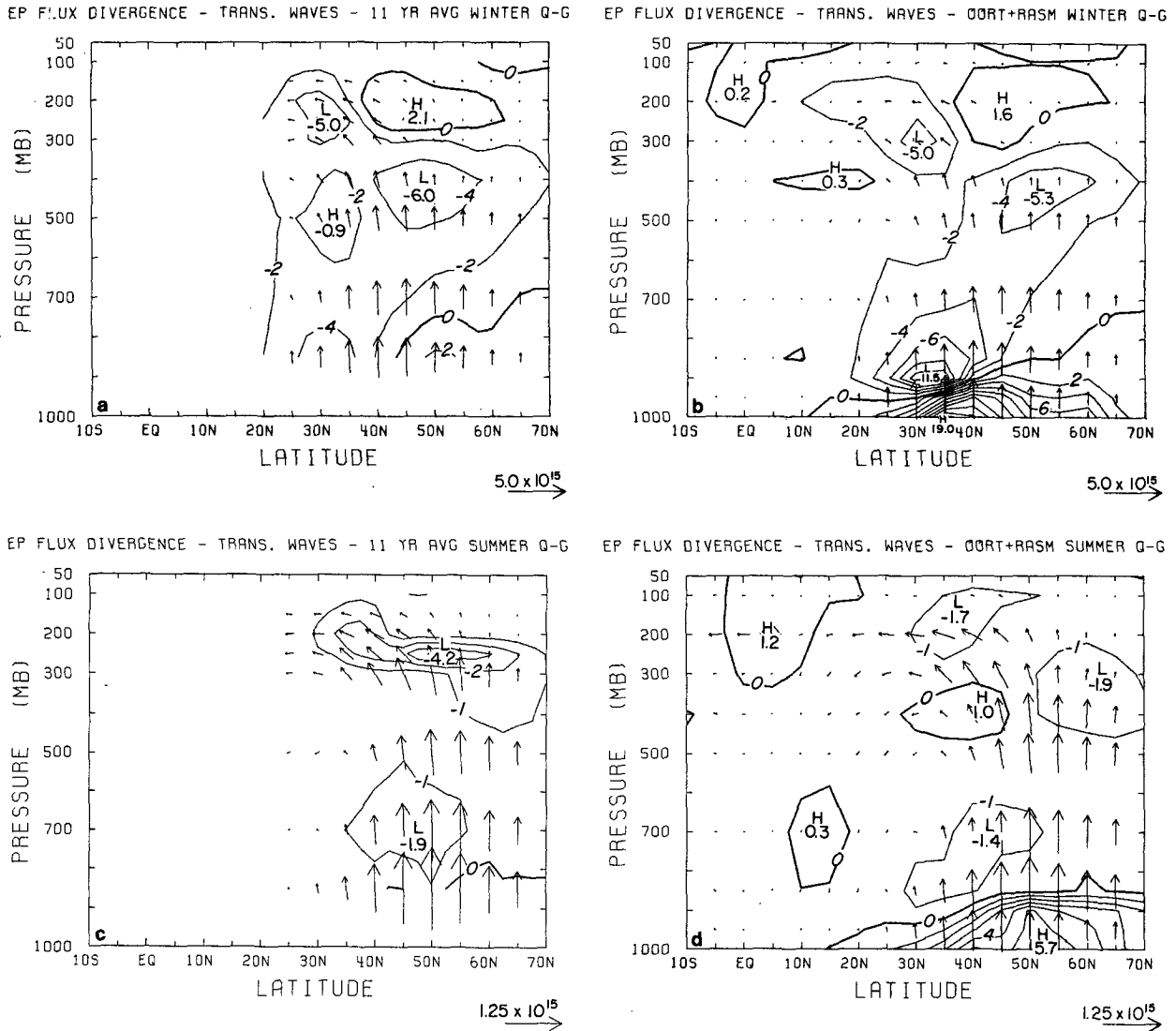


FIG. 1. Contribution of transient waves to seasonally averaged Eliassen-Palm cross sections for the troposphere: (a) 11-year average of NMC data for winter; (b) 5-year average from Oort and Rasmusson (1971) for winter; (c) and (d) the same, respectively, for summer. The NMC data used in (c) was kindly made available by G. H. White. The contour interval is  $2.0 \times 10^{15} \text{ m}^3$  for (a) and (b), and  $1.0 \times 10^{15} \text{ m}^3$  for (c) and (d). The horizontal arrow scale for  $\bar{F}_{(p)}$  in units of  $\text{m}^3$  is indicated at bottom right; note that it is different from diagram to diagram. A vertical arrow of the same length represents a flux  $\bar{F}_{(p)}$ , in  $\text{m}^3 \text{ kPa}$ , equal to that for the horizontal arrow multiplied by 80.4 kPa.

possibility that there were some real, systematic differences between the summers of 1958–62 and those of 1966–77 should not perhaps be dismissed altogether.

It is of interest to compare the winter pictures, especially, with the results from simple models of baroclinic waves. Fig. 2a shows the EP signature of a growing Eady mode in a channel. It has upward EP flux independent of height; thus  $\nabla \cdot \mathbf{F}$  is zero in the interior. Fig. 2b is for a maximally unstable Charney mode. In contrast to the Eady mode, its greatest EP flux is at the lower surface, decreasing to small values above the steering level or level at

which the zonal wind speed equals the wave speed, shown by a heavy line marked “s.l.” in the figure. The convergence is roughly independent of depth up to the steering level, but decreases rapidly above. A more complete picture is obtained by following Bretherton (1966) and regarding boundary potential-temperature gradients as concentrated gradients of quasi-geostrophic potential vorticity. In this viewpoint,  $F_{(p)}$  is taken as zero at the boundary but non-zero an infinitesimal distance from the boundary. The Eady mode then has concentrated divergence at the lower boundary and concentrated convergence at the upper boundary. Provided we thus take the



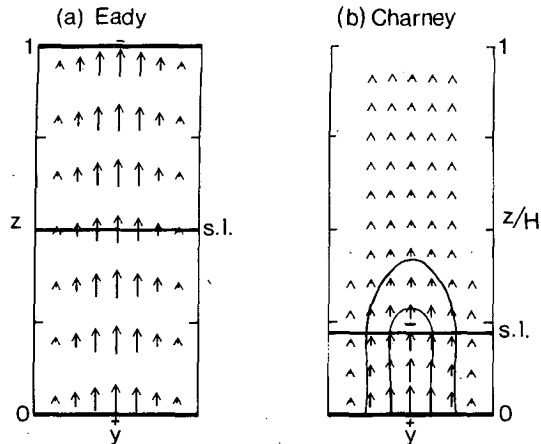


FIG. 2. Examples of Eliassen-Palm cross sections for linear baroclinic instabilities, from (a) Eady's theory and (b) Charney's theory. Steering levels are marked s.l. In (b),  $H$  is the density scale height, and the contours for  $\nabla \cdot \mathbf{F}$  have values  $-0.4$  and  $-0.8$  of the maximum. The thick horizontal boundaries are meant to suggest infinite crowding of  $\nabla \cdot \mathbf{F}$  contours representing concentrated divergence at the boundaries, positive at each lower boundary and negative in (a) at the upper boundary; see Eq. (4.1). The cross section for the Charney mode was sketched from a numerical solution kindly made available to us by B. Farrell. [It is somewhat similar to that in Fig. 10b of Lindzen *et al.* (1980), for a wide channel (width  $\gg$  zonal half-wavelength). If the channel width is diminished, the  $\nabla \cdot \mathbf{F}$  contours concentrate more and more closely around the steering level, as implied by McIntyre (1972, Fig. 2c) and in Lindzen *et al.* (1980, Fig. 10c).]

boundary contributions into account, the convergence and divergence must compensate exactly, in the sense that

$$\int_{\text{whole domain}} \nabla \cdot \mathbf{F} dm = 0 \quad (4.1)$$

by the divergence theorem. The Charney mode has divergence concentrated at the lower boundary, too, but most of the compensating convergence occurs around and below the steering level (Lindzen *et al.*, 1980). The concentrated divergence at the boundary correctly suggests the active role of the boundary in the instability mechanism.

Despite a more realistic mean state the EP cross section for the Charney mode fails to resemble the observed cross sections at all closely. A far better comparison with observation is obtained from numerically simulated life cycles of nonlinear baroclinic waves on the sphere. The particular example we shall quote is the most unstable zonal wave-number 6 disturbance to a jet at  $\sim 45^\circ$  latitude and 200 mb, with a realistically sloping tropopause. It is the basic case described in Simmons and Hoskins (1980, Fig. 1a). The linear mode for this jet, whose EP signature is shown in Fig. 3a, is quite similar to the Charney mode. The position of the steering level is again shown by a heavy line, curved this time

because of the mean jet. There is a weak secondary convergence maximum near the tropopause, faintly mimicking the Eady mode's upper convergence region. As the wave becomes nonlinear the principal convergence maximum moves away from the lower surface until by day 5, the time of maximum vertical flux  $F_{(p)}$ , there is divergence in a region near the surface as seen in Fig. 3b, and much stronger convergence aloft, more like the Eady mode. At day 6 (not shown) the maximum upward flux is at 700 mb and there is large divergence near the surface. At upper levels another phenomenon is becoming noticeable: the arrows are tilting toward the tropics, and the convergence region is extending equatorward along the tropopause. At day 8 (Fig. 3c) the equatorward flux is at a maximum. Growth has ceased and barotropic decay is starting.

The time-averaged picture over the life cycle is shown in Fig. 3d. Though the initial linear stage (Fig. 3a) resembles a Charney mode, the time-averaged pattern looks more similar, if anything, to that of an Eady mode. None of the linear modes, including that of Fig. 3a, produce the strong equatorward tilt of  $\mathbf{F}$  in the upper troposphere evident in Fig. 3d, nor the equatorward position of the main upper tropospheric convergence region. Those features are also evident in Figs. 1a and 1b. The planetary-wave propagation mechanism seems important here: it would produce much the same upward and equatorward fluxes from an initial, low-level, midlatitude disturbance created by *any* means [e.g., by the lower boundary—see Fig. 1a of Dunkerton *et al.* (1980)]. Planetary-wave radiation is weak during the linear, strongly growing stage of the instability, simply because the radiation has no time to develop until after growth slows down (Charney and Pedlosky, 1963; McIntyre and Weissman, 1978). But its subsequent development provides an important dynamical link between the low midlatitude and high subtropical troposphere (e.g., Dickinson, 1978, p. 176).<sup>5</sup>

Thus the EP cross sections bring out especially clearly the interplay of linear and nonlinear processes in the life cycle, and in particular the fact that eddy-flux parameterization schemes should not be based on linear baroclinic-instability theory. [Recall that the  $\nabla \cdot \mathbf{F}$  contour patterns directly indicate the net effect of the eddies on the mean state, by Eqs. (2.3) and (3.3).] The time-averaged nonlinear picture (Fig. 3d) comes much closer to imitating Figs.

<sup>5</sup> One consequence of the radiation mechanism [particularly its earliest, vertically upward phase (Fig. 3b)] is that the precise position of the steering level is not specially important for the overall, time-averaged signature of the life cycle (contrast Lindzen *et al.*, 1980, section 3e)—even though Figs. 2b and 3a remind us that the steering level's position is crucial for the structure of linear modes on realistic mean states (Lindzen *et al.*, 1980; McIntyre, 1972).

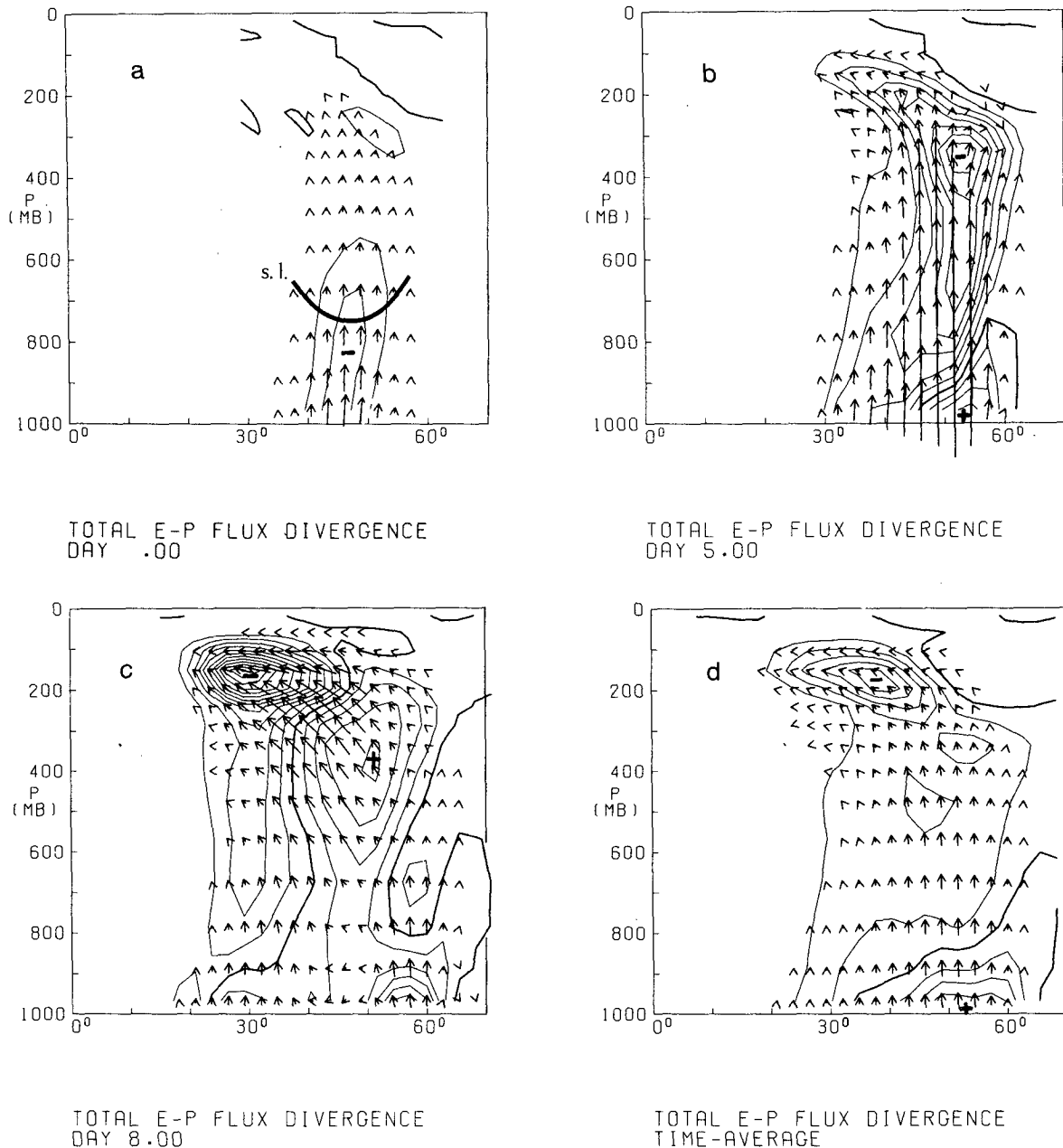


FIG. 3. (a) Eliassen-Palm cross section for a linear, growing baroclinic instability on a realistic mean state [the first case studied in Simmons and Hoskins (1980)]; (b), (c) cross sections for two stages in the life cycle of the same disturbance after it goes nonlinear; (d) time-averaged cross section for the life cycle. The contour interval is  $4 \times 10^{15} \text{ m}^3$  for (b) and (c), and  $1.5 \times 10^{15} \text{ m}^3$  for (d). The arrow scales are the same in all three, and such that the distance occupied by  $10^\circ$  of latitude represents a value  $12.5 \times 10^{15} \text{ m}^3$  of  $\bar{F}_{(p)}$ , and that occupied by 100 mb represents a value  $7150 \times 10^{15} \text{ m}^3 \text{ mb}$ , or  $715 \times 10^{15} \text{ m}^3 \text{ kPa}$ , of  $\bar{F}_{(p)}$ .

1a and 1b than does any of the linear pictures, the main differences being in the subtropical lower troposphere between  $25$  and  $40^\circ\text{N}$ , where the static stability is low (especially if the effect of moisture is considered), and also at  $\sim 50^\circ\text{N}$  and  $450 \text{ mb}$  where a strong convergence feature in Figs. 1a and 1b is only weakly echoed in Fig. 3d. One reason for the latter discrepancy could be the model's suppression

of baroclinic instability toward polar regions, due to the restriction to zonal wavenumber 6 and its harmonics; another might be diabatic effects omitted from the model (see Section 5).

By Eq. (3.5), the pattern of  $\nabla \cdot \mathbf{F}$  is also that of the northward quasi-geostrophic potential-vorticity flux  $v'q'$ . The predominantly negative values of  $\nabla \cdot \mathbf{F}$  in Figs. 1 and 3d indicate downgradient potential-

vorticity fluxes for the most part, since the local mean gradient  $\bar{q}_\phi$  is positive throughout much of the troposphere. A temporary upgradient flux is prominent in Fig. 3c at 50°N and 400 mb, presumably caused by locally decaying disturbance amplitude (Rhines and Holland, 1979). The *time-averaged*  $\overline{v'q'}$  is still downgradient there, as we might expect from the ideas reviewed in Section 2b.

A net positive  $\overline{v'q'}$  remains near the bottom of the time-averaged model picture, and is seen also in the observed pictures. This may be viewed as part of the occlusion process. The decrease in meridional temperature gradient and increase in static stability at low levels makes the term  $f(\partial_\phi/\partial_p)$  in the expression (3.8) for  $\bar{q}_\phi$  strongly negative. Positive values of low-level  $\overline{v'q'}$  first appear at day 5 in a region where  $\bar{q}_\phi$  has just become very small or negative. The coincidence of mostly negative  $\bar{q}_\phi$  with positive  $\overline{v'q'}$  remains true during days 6 and 7 when the values of  $\overline{v'q'}$  are at their largest. In the time average,  $\bar{q}_\phi$  is negative only from 60 to 74°, but this is clearly not a reflection of the flow when the positive  $\overline{v'q'}$  is generated. With  $\bar{q}_\phi$  small, it is also probable that frictional and diabatic effects have a significant influence on the sign of  $\overline{v'q'}$ , especially where dissipation associated with frontogenesis and occlusion as well as the boundary layer may be important. Andrews and McIntyre (1976) have given examples where the term  $D$  in (2.12) can have either sign, depending on dissipation mechanism and eddy structure.

The wintertime lower stratosphere around 50°N and 200 mb is another region exhibiting positive  $\nabla \cdot \mathbf{F}$  values, especially in the observational cross sections. The fact that they appear in both Figs. 1a and 1b suggests that they could be real despite rather small magnitudes. We think that in this region the positive  $\nabla \cdot \mathbf{F}$  values are also likely to be indicative of negative  $\bar{q}_\phi$ . The idea is first of all consistent with the fact that stationary disturbances cannot by themselves cause irreversible air-parcel dispersion; and their EP cross sections, to be presented shortly, show no sign of positive  $\nabla \cdot \mathbf{F}$  values in the same region. A stronger and more direct line of evidence comes from some calculations by Mahlman (1966), of Ertel's potential vorticity in the 400 K isentropic surface. The northward gradient of this quantity is approximately equal to that of  $q$  (Charney and Stern, 1962). In typical winter months (but not in summer), Mahlman found negative gradients in about the right latitudes, where the 400 K surface was at  $\sim 100$  mb.

The corresponding feature in Fig. 3d is much weaker, but does definitely seem to be associated with negative  $\bar{q}_\phi$ . At each day before day 8 the only region of positive  $\overline{v'q'}$  above the lower troposphere coincides almost exactly with the only region of weak negative values of  $\bar{q}_\phi$ . Diabatic effects seem

unlikely to be large enough to be important at these altitudes; radiative relaxation times in the lower stratosphere are slow compared to the dynamical time scales of the events summarized by Fig. 3. However, we did check this by rerunning the simulation with a Newtonian cooling added whose e-folding time constant was 5 days. Even such an unrealistically strong Newtonian cooling had a negligible effect on the model EP cross sections, which were virtually indistinguishable from those of Fig. 3.

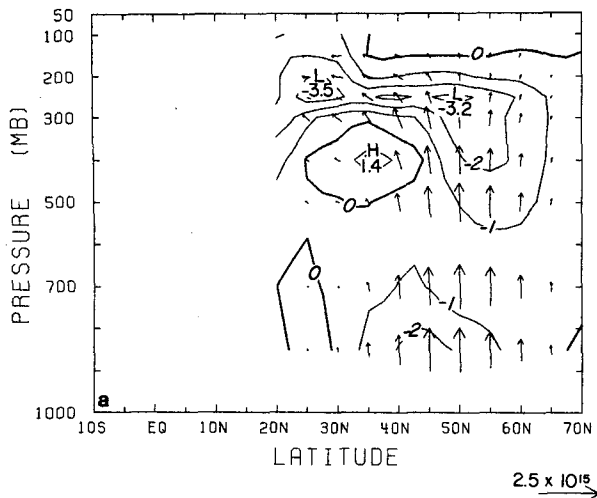
It is natural to ask why, in fact, the lower stratospheric region of positive  $\nabla \cdot \mathbf{F}$  is relatively much stronger in Figs. 1a and 1b than in Fig. 3d. It is again likely that the model may simply be excluding some of the instability modes contributing to Figs. 1a and 1b. The weak lower stratospheric baroclinic instabilities pointed out by McIntyre (1972), and further discussed by Simmons (1972) and Holton (1975), are one obvious candidate.

## 5. Stationary eddies

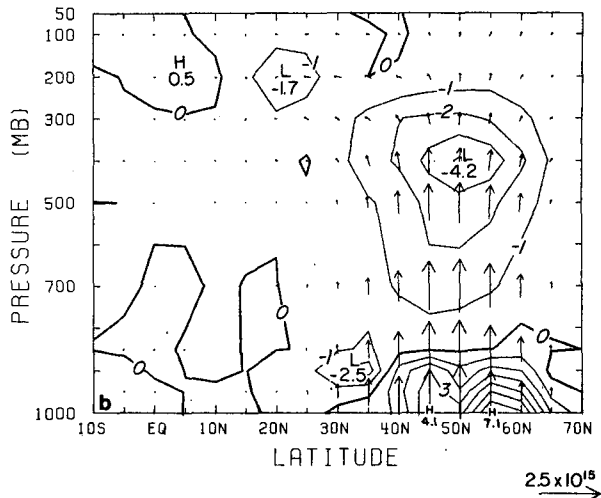
The stationary counterparts of Figs. 1a–1d are presented in Figs. 4a–4d. The wintertime arrows in Figs. 4a and 4b are smaller in magnitude than their transient counterparts. The arrow patterns look broadly similar: most of the arrows in Figs. 4a and 4b display the same tendency to tilt equatorward toward the high subtropical troposphere. The main difference between the stationary and transient wintertime arrow patterns appears at high altitudes in middle and high latitudes, where upward radiation of ultralong planetary waves into the stratosphere is evidently making a noticeable contribution. [The contribution from zonal wavenumber 1 alone is of the right order to account for the sizes of the vertical arrows at 50°N upwards of 200 mb, if we estimate it from Figs. 2 and 10 of van Loon *et al.* (1973).]

Of course there are mechanisms quite different from wave propagation which can contribute to  $F_{(p)}$ , especially for large-scale, stationary eddies in the troposphere where we would expect substantial fluctuations  $\theta'$  in potential temperature to be induced diabatically. If diabatic heating (redistributed in the vertical by ageostrophic eddy heat transports) is such that an air mass is being heated while *displaced* southward, so that it is *relatively warm* when *traveling* northward, and so on, then  $v'\theta'$ , of course, will tend to be positive quite independently of wave propagation or other processes describable in terms of adiabatic motion. In Eq. (2.12) this is a straightforward manifestation of the  $D$  term. The magnitude of the effect should decrease as we move into the upper troposphere, tending to give negative  $\nabla \cdot \mathbf{F}$  in mid-troposphere as observed in Figs. 4a and 4b. A similar diabatic effect might contribute to the mid-tropospheric convergence feature already noted

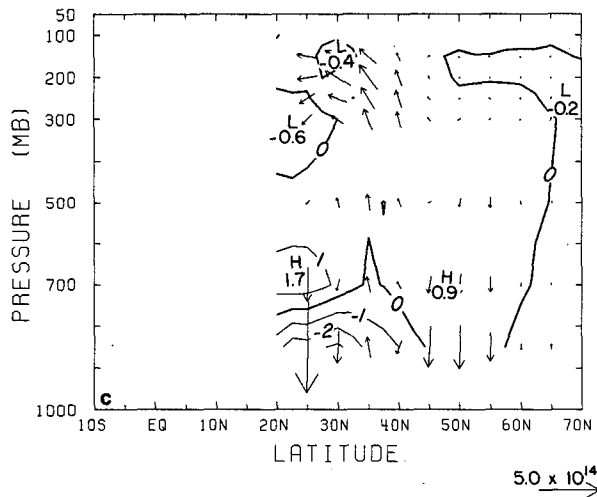
EP FLUX DIVERGENCE - STAT. WAVES - 11 YR AVG WINTER Q-G



EP FLUX DIVERGENCE - STAT. WAVES - OORT+RASM WINTER Q-G



EP FLUX DIVERGENCE - STAT. WAVES - 11 YR AVG SUMMER Q-G



EP FLUX DIVERGENCE - STAT. WAVES - OORT+RASM SUMMER Q-G

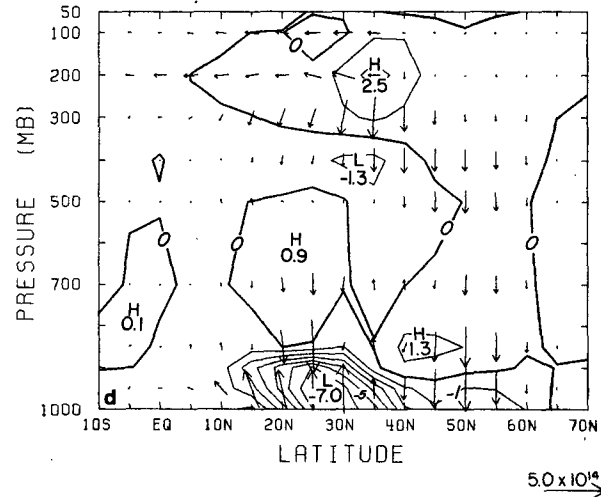


FIG. 4. Contribution of stationary waves to seasonally averaged Eliassen-Palm cross sections for the troposphere: (a) 11-year average of NMC data for winter; (b) 5-year average from Oort and Rasmusson (1971) for winter; (c) and (d): the same, respectively, for summer. The contour interval is  $1.0 \times 10^{15} \text{ m}^3$  for all four panels. The horizontal arrow scale in units of  $\text{m}^3$  is indicated at bottom right.

around  $50^\circ\text{N}$  in the transient cross sections of Figs. 1a and 1b.

However, the detailed  $\nabla \cdot \mathbf{F}$  patterns are too different between Figs. 4a and 4b to inspire great confidence in their statistical stability. This may be inevitable in view of the problems of geographical bias, which are obviously worse for stationary eddy statistics than for transient ones—although we should still not forget the possibility that there might have been differences in the actual behavior of the atmosphere between the years 1958–63 and 1965–76.

The problems of data noise and bias are most severe of all for the summer stationary-wave patterns in Figs. 4c and 4d (note the small numerical

values). Despite these limitations, the differences between the winter and summer cross sections are intriguing, and invite some brief speculation. Common to Figs. 4c and 4d are signs of an apparent source of EP flux in the upper troposphere in middle latitudes. This is noteworthy, if real, because it is not predicted by any of the usual linear models of orographic and thermal forcing of planetary waves (e.g., Shutts, 1978, p. 347).

A net upper tropospheric source of EP flux associated with stationary planetary waves could arise from at least two possible causes. One, suggested by Dickinson (1971; 1978, p. 176), is deep convection, especially that associated with the Asian mon-

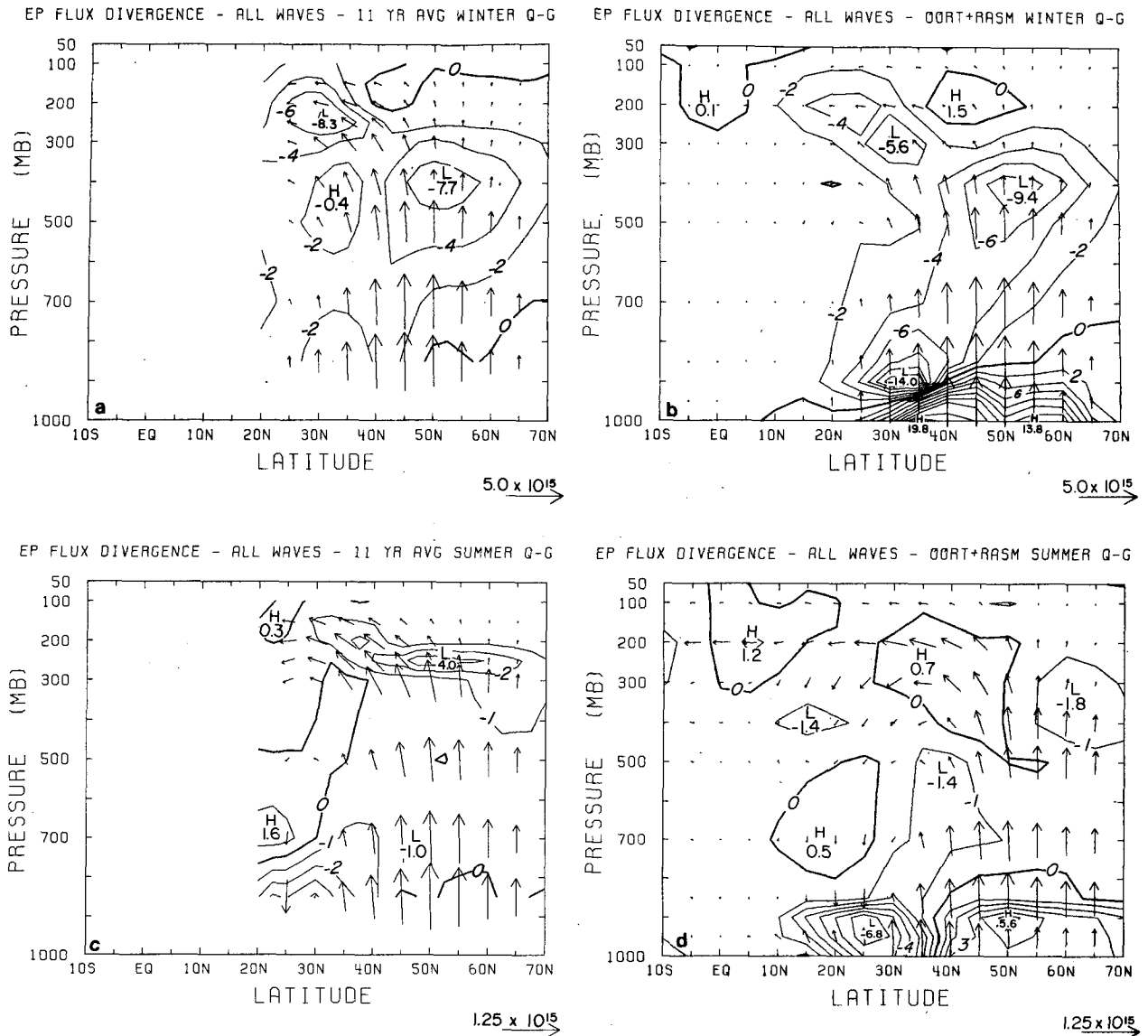


FIG. 5. Total (transient plus stationary) Eliassen-Palm cross sections for the troposphere: (a) 11-year average of NMC data for winter; (b) 5-year average from Oort and Rasmusson (1971) for winter; (c) and (d): the same, respectively, for summer. The contour interval is  $2.0 \times 10^{15} \text{ m}^3$  for (a) and (b), and  $1.0 \times 10^{15} \text{ m}^3$  for (c) and (d). The horizontal arrow scale in units of  $\text{m}^3$  is indicated at bottom right.

soon and orographic uplift by the Himalayas. Whether the associated diabatic effects could produce a pattern like that in Fig. 4c, for instance, is not obvious without model calculations yet to be done. The second possibility is the nonlinear interaction between transient and stationary waves. (Note the hint of complementarity between Figs. 4c and 1c and recall the nonlinear EP theorem; note also, by way of caution, that many other processes must be occurring and that our EP cross sections are a statistical residual of all these.) Again, modeling studies would be a good way of testing the idea.

## 6. The general circulation in terms of the transformed mean equations

Figs. 5a–5d are the EP cross sections for transient and stationary eddies taken together, i.e., the result of adding Figs. 1a–1d and 4a–4d. The winter cross sections (Figs. 5a and 5b) agree as to their main features, the summer cross sections less so. The contours in Figs. 5a–5d give observational estimates of the total eddy-induced torque on the zonal-mean atmosphere. The meridional circulation which arises as a response to this is the *residual* meridional circu-

lation appearing in the transformed mean equations (3.3) and (3.9).

Fig. 6 shows the winter and summer streamfunctions  $\bar{\psi}^*$  defined by

$$\bar{v}^* = (g/2\pi r_0^2 \cos\varphi)\bar{\psi}_v^*, \quad (6.1a)$$

$$\bar{\omega}^* = -(g/2\pi r_0^3 \cos\varphi)\bar{\omega}_\varphi^*, \quad (6.1b)$$

according to Oort and Rasmusson's data, which covers a more extensive range of heights and latitudes and is therefore more suitable for computing the streamfunctions. (The NMC data are not suitable, if only because they do not describe the tropical Hadley cell.) Because of the inaccuracies in the raw zonally averaged meridional velocities in Oort and Rasmusson's Table A2, especially with regard to the strength of the Ferrel cell in  $\bar{v}$ , the balanced meridional velocities (their Table F3) were used to calculate the values of  $\bar{v}^*$ . Since there is no reason to expect  $\bar{\omega}^*$  to be zero at sea level,<sup>6</sup> Eq. (6.1a) was integrated downward from the highest data level (50 mb). As a check we also integrated (6.1b) northward from 10°S and the result was very similar. Fig. 6 gives the average of the two integrations.

In a statistically steady state, the effect of the torque  $\nabla \cdot \mathbf{F}$ , as modified by the term  $r_0^{-1}\bar{v}^*M_\varphi$  in (3.9), must be balanced by "friction"  $r_0 \cos\varphi \cdot \mathcal{F}$ —provided we define the latter to mean the sum of all the ageostrophic and small-scale contributions to the angular momentum budget not explicitly represented in Eq. (3.9). We find that  $\mathcal{F}$  is small compared to  $\nabla \cdot \mathbf{F}$  and  $r_0^{-1}\bar{v}^*M_\varphi$ , and well within the noise of the data, except in the planetary boundary layer. The near-cancellation between  $\nabla \cdot \mathbf{F}$  and  $r_0^{-1}\bar{v}^*M_\varphi$  is related to the near-cancellation between  $(\overline{u'v'})_y$  and  $f\bar{v}$  familiar in the standard Eulerian-mean description of the general circulation. It thus turns out that, above the boundary layer, we can estimate the residual meridional circulation just as well from  $\nabla \cdot \mathbf{F}$ , simply by setting  $\partial M/\partial t$  and  $\mathcal{F}$  equal to zero in (3.9). This gives pictures (not shown) which are very similar to Figs. 6a and 6b in the midlatitude free atmosphere.

Eqs. (3.3c,d) show that in a steady state the residual circulation may equally well be regarded as a response to the net heating  $\bar{Q}$ . As before, it is best to define  $\bar{Q}$  to include all ageostrophic terms not explicitly represented in (3.3d), as well as all diabatic effects. Among such ageostrophic terms is

<sup>6</sup> The same is true of the meridional circulation calculated by Sasamori (1978) (contrary to an assumption in that paper); it is equal to the residual circulation for stationary waves plus the full Eulerian-mean circulation for transient waves minus a term representing the Hadley circulation. The standard Eulerian-mean streamfunction  $\bar{\psi}$  is not quite zero at sea level either, for that matter, if only because of topographical effects (Uryu, 1974; Bretherton and Haidvogel, 1976; Andrews, 1980; McIntyre, 1980b).

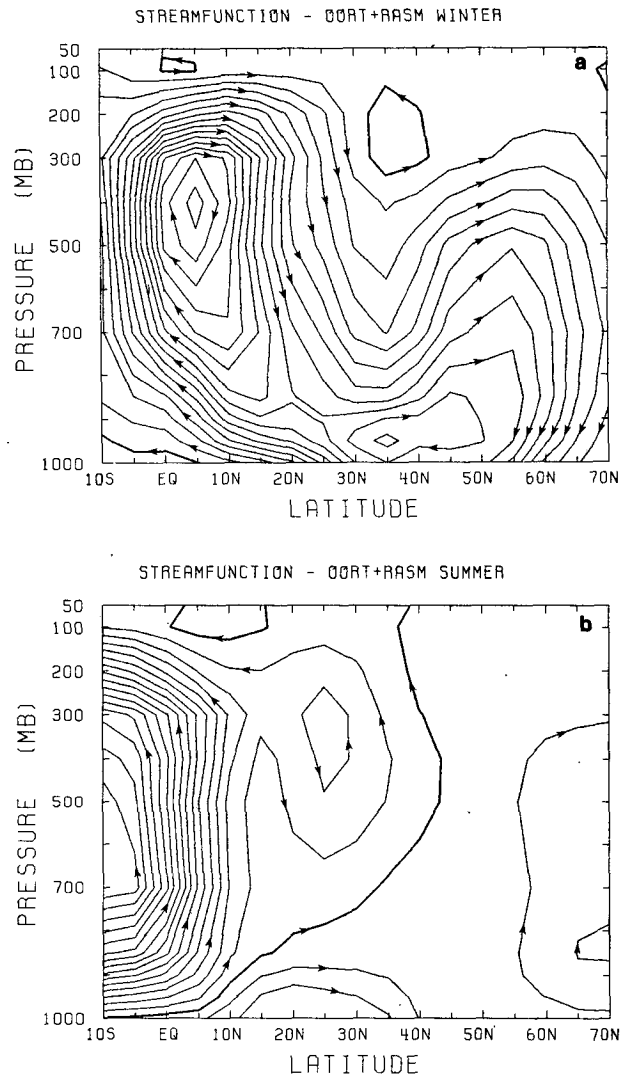


FIG. 6. Seasonally averaged residual meridional circulations. The streamfunction is defined by Eqs. (6.1): (a) 5-year average from Oort and Rasmusson (1971) for winter and (b) the same for summer. The contour interval is  $7.5 \times 10^{16} \text{ m}^2 \text{ s Pa}$ .

the divergence of the vertical eddy flux of heat, which as already mentioned has been found to play a significant role in the nonlinear evolution of baroclinic waves (e.g., Simmons and Hoskins, 1978). Order-of-magnitude estimates suggest that in mid-latitudes it is comparable to the net diabatic heating, both being roughly of the order of  $1 \text{ K day}^{-1}$ .

This fact seems to be important for understanding the shape of the wintertime streamline pattern in Fig. 6a, particularly the rising branch indicating positive values of  $\bar{Q}$  throughout a deep layer in middle latitudes. Fig. 10a of Simmons and Hoskins (1978) suggests that this can be largely accounted for in terms of latent heat released at low levels and then transported upward (in the Eulerian sense) by midlatitude baroclinic disturbances. [The rising

branch in Fig. 6a is therefore *not* a feature which should occur in a Lagrangian-mean meridional circulation. Kida's (1977) computations of such a circulation in a model troposphere show downward motion throughout middle latitudes, much as we would expect.]

The remaining features in Fig. 6a and 6b accord with familiar ideas (e.g., Newell *et al.*, 1974, Figs. 6.11, 7.16, 7.17, 7.18 and 7.22). In our Fig. 6a, the rising branch of the Hadley cell just south of the equator represents the net effect of deep convective heating together with vertical eddy heat fluxes on cloud-cluster scales. Near 20°N in Fig. 6a we have low-level convective heating below the trade inversion, and infrared radiative cooling in the free atmosphere. Near 60°N infrared cooling again dominates in the free atmosphere, but boundary-layer processes over the continents produce net cooling at low levels as well.

In summer (Fig. 6b), the main Hadley-cell heating is further north, and elsewhere there appears to be cancellation between boundary layer heating, latent heat release at lower levels, infrared cooling at upper levels, and upward transport by the eddies.

### 7. EP cross sections extending over many scale heights

The data sets used in this study give a tantalizing glimpse of the lower stratosphere, but not higher up. EP cross sections would appear to be a very natural way of describing the net flow of planetary-wave activity through the stratosphere. They should be the clearest means, for instance, of displaying the observational evidence for or against absorption of stationary planetary waves near zero-wind lines. A start on the observational problem has been made by Palmer (1980) and Sato (1980).

There is, however, a dilemma concerning scales for the arrows to be used in EP cross sections extending over many scale heights. The only practicable vertical coordinate for such pictures is  $\log p$ , geometrical height, or something similar. If  $\log p$  replaces  $p$  in the diagrams, we must write  $dp$  in (3.10) as  $p d(\log p)$ , and insert factors  $p$  into the first component of (3.13) and into the definition (3.12) of  $\Delta$ . With these redefinitions we have

$$\Delta = \frac{\partial \hat{F}_{(\varphi)}}{\partial \varphi} + \frac{\partial \hat{F}_{(p)}}{\partial (\log p)}, \quad (7.1)$$

and the pattern of arrows will again look nondivergent when and only when  $\nabla \cdot \mathbf{F} = 0$ .

If we had a constant upward flux of wave activity, with eddy velocities increasing like the inverse square root of density, then the arrow lengths, so defined, would be constant with height. However, in the real atmosphere such an unattenuated wave flux never persists over many scale heights, since dissipation of some kind or another is bound to build

up as soon as eddy velocities  $u'$  become comparable with intrinsic zonal phase velocities  $\hat{c}$ . In practice the flux will drop off with height and a true EP cross section, as defined here, will tend to emphasize events lower down—perfectly correctly in terms of absolute values of, say, angular momentum in Eq. (3.9), but not usefully in terms of the local order of magnitude of, say,  $u'/\hat{c}$ .

There is no reason why  $\Delta$  should not be multiplied by any desired function of altitude before plotting its contours. But the dilemma is real for the arrows since although rescaling them by a function of  $\log p$  will preserve their directions, it will make them appear divergent when  $\nabla \cdot \mathbf{F} = 0$ . In most cases it will probably be best to put up with this anomaly, and rely on the contours of  $\nabla \cdot \mathbf{F}$  as the sole indicator of divergence. The arrows would then be there purely to indicate flux directions, and relative flux magnitudes at each altitude.

### 8. Concluding remarks

EP cross sections and the transformed mean-flow equations furnish a powerful and practical way of viewing the dynamics of eddies on a zonal wind, whether in the troposphere or in the middle atmosphere, and whether or not the eddies are well described by linear wave theory. Recall particularly the nonlinear version of the quasi-geostrophic EP theorem noted in Section 2c, and the absence of geostrophic eddy-heat-flux terms from the transformed mean equations (2.3) and (3.3). The information displayed on an EP cross section comes as close to the heart of the eddy, mean-flow interaction problem as seems likely to be possible for any Eulerian diagnostic. We again emphasize that these diagnostics exploit the theoretical concepts in such a way as not to depend on the restrictive assumptions originally made by Eliassen and Palm (1961) and Charney and Drazin (1961).

For the troposphere it would be of great interest to see the EP cross sections for different zonal wavenumbers (for example, to test some of the suggestions in Section 5). Individual days would be of interest as well as seasonal averages. If such cross sections could be obtained despite the formidable data-quality problems, they would give a revealing view of the horizontal, vertical and temporal structure of the interactions among different kinds of eddy and the zonal-mean state. Such questions could certainly be studied by means of general circulation models, and by means of less complex models like those of Gall *et al.* (1979) and Frederiksen (1980). Another area which we have had to leave untouched is that of accounting for the stationary-wave cross sections of Fig. 4; it is not clear at present how sophisticated a model of tropospheric stationary waves would be needed to produce the main features of, say, the wintertime cross sections of Figs. 4a and b.

**Acknowledgments.** We thank D. G. Andrews, B. Farrell, Y. Hayashi, I. Held, J. R. Holton, C.-P. Hsu, N.-C. Lau, J. Mahlman, T. N. Palmer, R. L. Pfeffer, J. M. Wallace and G. H. White for help and suggestions. HJE's and MEM's research was supported by the Joint Institute for the Study of the Atmosphere and Ocean, funded by the University of Washington and the National Oceanographic and Atmospheric Administration under Contract 03-7-022-35211. BJH's research was supported by the Natural Environment Research Council and the University of Reading.

## REFERENCES

- Andrews, D. G., 1980: On the mean motion induced by transient inertio-gravity waves. *Pure Appl. Geophys.*, **118**, 177-188.
- , and M. E. McIntyre, 1976: Planetary waves in horizontal and vertical shear: the generalized Eliassen-Palm relation and the mean zonal acceleration. *J. Atmos. Sci.*, **33**, 2031-2048.
- , and —, 1978a: Generalized Eliassen-Palm and Charney-Drazin theorems for waves on axisymmetric flows in compressible atmospheres. *J. Atmos. Sci.*, **35**, 175-185.
- , and —, 1978b: An exact theory of nonlinear waves on a Lagrangian-mean flow. *J. Fluid Mech.*, **89**, 609-646.
- Benney, D. J., and R. F. Bergeron, 1969: A new class of nonlinear waves in parallel flows. *Stud. Appl. Math.*, **48**, 181-204.
- Blackmon, M. L., 1976: A climatological spectral study of the 500 mb geopotential height of the Northern Hemisphere. *J. Atmos. Sci.*, **33**, 1607-1623.
- , J. M. Wallace, N.-C. Lau and S. L. Martin, 1977: An observational study of the Northern Hemisphere wintertime circulation. *J. Atmos. Sci.*, **34**, 1040-1053.
- Boyd, J., 1976: The noninteraction of waves with the zonally averaged flow on a spherical earth and the interrelationships of eddy fluxes of energy, heat and momentum. *J. Atmos. Sci.*, **33**, 2285-2291.
- Bretherton, F. P., 1966: Critical layer instability in baroclinic flows. *Quart. J. Roy. Meteor. Soc.*, **92**, 325-334.
- , and D. B. Haidvogel, 1976: Two-dimensional turbulence above topography. *J. Fluid Mech.*, **78**, 129-154 [see Eq. (53)].
- Charney, J. G., and P. G. Drazin, 1961: Propagation of planetary-scale disturbances from the lower into the upper atmosphere. *J. Geophys. Res.*, **66**, 83-109.
- , and J. Pedlosky, 1963: On the trapping of unstable planetary waves in the atmosphere. *J. Geophys. Res.*, **68**, 6441-6442.
- , and M. E. Stern, 1962: On the stability of internal baroclinic jets in a rotating atmosphere. *J. Atmos. Sci.*, **19**, 159-172.
- Davis, R. E., 1969: On the high Reynolds number flow over a wavy boundary. *J. Fluid Mech.*, **36**, 337-346.
- Dickinson, R. E., 1969: Theory of planetary wave-zonal flow interaction. *J. Atmos. Sci.*, **26**, 73-81.
- , 1971: Cross-equatorial eddy momentum fluxes as evidence of tropical planetary wave sources. *Quart. J. Roy. Meteor. Soc.*, **97**, 554-558.
- , 1978: Rossby waves—long-period oscillations of oceans and atmospheres. *Annual Review of Fluid Mechanics*, Vol. 10, Annual Reviews, Inc., 159-195.
- Dunkerton, T. J., 1980: A Lagrangian-mean theory of wave, mean-flow interaction with applications to nonacceleration and its breakdown. *Revs. Geophys. Space Phys.*, **18**, 387-400.
- , 1978: On the mean meridional mass motions of the stratosphere and mesosphere. *J. Atmos. Sci.*, **35**, 2325-2333.
- , C.-P. Hsu and M. E. McIntyre, 1980: Some Eulerian and Lagrangian diagnostics for a model stratospheric warming. Submitted to *J. Atmos. Sci.*
- Eliassen, A., 1952: Slow thermally or frictionally controlled meridional circulation in a circular vortex. *Astrophys. Nørveg.*, **5**, No. 2, 19-60.
- , and E. Palm, 1961: On the transfer of energy in stationary mountain waves. *Geophys. Publ.*, **22**, No. 3, 1-23.
- Frederiksen, J. S., 1980: Zonal and meridional variations of eddy fluxes induced by long planetary waves. *Quart. J. Roy. Meteor. Soc.*, **106**, 63-84.
- Gail, R., R. Blakeslee and R. C. J. Somerville, 1979: Cyclone-scale forcing of ultralong waves. *J. Atmos. Sci.*, **36**, 1692-1698.
- Geisler, J. E., 1974: A numerical model of the sudden stratospheric warming mechanism. *J. Geophys. Res.*, **79**, 4989-4999.
- Green, J. S. A., 1970: Transfer properties of the large-scale eddies and the general circulation of the atmosphere. *Quart. J. Roy. Meteor.*, **96**, 157-185.
- Hartmann, D. L., 1977: On potential vorticity and transport in the stratosphere. *J. Atmos. Sci.*, **34**, 968-977.
- Hayes, M., 1977: A note on group velocity. *Proc. Roy. Soc. London*, **354**, 533-535.
- Holton, J. R., 1975: *The Dynamic Meteorology of the Stratosphere and Mesosphere*. Meteor. Monogr., No. 37, Amer. Meteor. Soc., 218 pp.
- , and T. Dunkerton, 1978: On the role of wave transience and dissipation in stratospheric mean flow vacillations. *J. Atmos. Sci.*, **35**, 740-744.
- , and W. M. Wehrbein, 1980: The role of forced planetary waves in the annual cycle of the zonal mean circulation of the middle atmosphere. *J. Atmos. Sci.*, **37**, 1968-1983.
- Kida, H., 1977: A numerical investigation of the atmospheric general circulation and stratospheric-tropospheric mass exchange: II. Lagrangian motion of the atmosphere. *J. Meteor. Soc. Japan*, **55**, 71-88.
- Lau, N.-C., 1978: On the three-dimensional structure of the observed transient eddy statistics of the Northern Hemisphere wintertime circulation. *J. Atmos. Sci.*, **35**, 1900-1923.
- , 1979a: The structure and energetics of transient disturbances in the Northern Hemisphere wintertime circulation. *J. Atmos. Sci.*, **36**, 982-995.
- , 1979b: The observed structure of tropospheric stationary waves and the local balances of vorticity and heat. *J. Atmos. Sci.*, **36**, 996-1016.
- , and J. M. Wallace, 1979: On the distribution of horizontal transports by transient eddies in the Northern Hemisphere wintertime circulation. *J. Atmos. Sci.*, **36**, 1844-1861.
- , H. Tennekes and J. M. Wallace, 1978: Maintenance of the momentum flux by transient eddies in the upper troposphere. *J. Atmos. Sci.*, **35**, 139-147.
- Lighthill, M. J., 1978: *Waves in Fluids*. Cambridge University Press, 504 pp.
- Lilly, D. K., 1972: Wave momentum flux—a GARP problem. *Bull. Amer. Meteor. Soc.*, **53**, 17-23.
- Lindzen, R. S., B. Farrell and K.-K. Tung, 1980: The concept of wave overreflection and its application to baroclinic instability. *J. Atmos. Sci.*, **37**, 44-63.
- Longuet-Higgins, M. S., 1964: On group velocity and energy flux in planetary wave motions. *Deep-Sea Res.*, **11**, 35-42.
- Mahlman, J. D., 1966: Atmospheric general circulation and transport of radioactive debris. Atmos. Sci. Pap. No. 103, Colorado State University. [The relevant information is reproduced as Fig. 3 of McIntyre (1972).]
- Matsuno, T., 1980: Lagrangian motion of air parcels in the stratosphere in the presence of planetary waves. *Pure Appl. Geophys.*, **118**, 189-216.
- McIntyre, M. E., 1972: Baroclinic instability of an idealized model of the polar night jet. *Quart. J. Roy. Meteor.*, **98**, 165-174.



- , 1980a: Towards a Lagrangian-mean description of stratospheric circulations and chemical transports. *Phil. Trans. Roy. Soc. London*, **A296**, 129–148.
- , 1980b: An introduction to the generalized Lagrangian-mean description of wave, mean-flow interaction. *Pure Appl. Geophys.*, **118**, 152–176.
- , and M. A. Weissman, 1978: On radiating instabilities and resonant overreflection. *J. Atmos. Sci.*, **35**, 1190–1196.
- Newell, R. E., J. W. Kidson, D. G. Vincent and G. J. Boer, 1974: *The General Circulation of the Tropical Atmosphere*, Vol. II. The MIT Press, 371 pp.
- Oort, A. H., and E. M. Rasmusson, 1971: Atmospheric circulation statistics. NOAA Prof. Pap. 5, U.S. Dept. of Commerce, Washington, DC, 323 pp.
- Palmer, T. N., 1981: Diagnostic study of a wavenumber-2 stratospheric sudden warming in the transformed Eulerian-mean formalism. *J. Atmos. Sci.*, **38** (in press).
- Plumb, R. A., 1979: Eddy fluxes of conserved quantities by small-amplitude waves. *J. Atmos. Sci.*, **36**, 1699–1704.
- Rhines, P. B., 1977: The dynamics of unsteady currents. *The Sea: Ideas and Observations on Progress in the Study of the Seas*, E. D. Goldberg et al., Eds., Wiley, Vol. 6, 189–318.
- , and W. R. Holland, 1979: A theoretical discussion of eddy-driven mean flows. *Dyn. Atmos. Oceans*, **3**, 289–325.
- Sasamori, T., 1978: A parameterization of large-scale heat transport in mid-latitudes. Part II. Stationary waves and the Ferrel cell. *Tellus*, **30**, 300–312.
- Sato, Y., 1980: Observational estimates of Eliassen and Palm flux due to quasi-stationary planetary waves. *J. Meteor. Soc. Japan* (in press).
- Shutts, G. J., 1978: Quasi-geostrophic planetary wave forcing. *Quart. J. Roy. Meteor. Soc.*, **104**, 331–350.
- Simmons, A. J., 1972: Baroclinic instability and planetary waves in the polar stratosphere. Ph.D. thesis, University of Cambridge.
- , and Hoskins, B. J., 1978: The life cycles of some nonlinear baroclinic waves. *J. Atmos. Sci.*, **35**, 414–432.
- , and —, 1980: Barotropic influences on the growth and decay of nonlinear baroclinic waves. *J. Atmos. Sci.*, **37**, 1679–1684.
- Taylor, G. I., 1915: Eddy motion in the atmosphere. *Phil. Trans. Roy. Soc. London*, **A215**, 1–26.
- Uryu, M., 1974: Induction and transmission of mean zonal flow by quasi-geostrophic disturbances. *J. Meteor. Soc. Japan*, **52**, 341–363.
- van Loon, H., R. L. Jenne and K. Labitzke, 1973: Zonal harmonic standing waves. *J. Geophys. Res.*, **78**, 4463–4471.
- Wallace, J. M., 1978: Trajectory slopes, countergradient heat fluxes and mixing by lower stratospheric waves. *J. Atmos. Sci.*, **35**, 554–558.